Chemical Science

RSC Publishing

EDGE ARTICLE

View Article Online
View Journal | View Issue

Cite this: *Chem. Sci.*, 2013, **4**, 3725

Fluorescent pH sensor constructed from a heteroatom-containing luminogen with tunable AIE and ICT characteristics†

Zhiyong Yang,[ab] Wei Qin,[ab] Jacky W. Y. Lam,[ab] Sijie Chen,[ab] Herman H. Y. Sung,[b] Ian D. Williams[b] and Ben Zhong Tang*[abc]

Received 8th March 2013
Accepted 5th July 2013

DOI: 10.1039/c3sc50648g

www.rsc.org/chemicalscience

A heteroatom-containing organic fluorophore 1-(4-pyridinyl)-1-phenyl-2-(9-carbazolyl)ethene (CP_3E) was designed and synthesized. CP_3E exhibits the effect of intramolecular charge transfer (ICT) caused by the donor–acceptor interaction between its carbazole and pyridine units. Whereas it emits faintly in solution, it becomes a strong emitter in the aggregated state, demonstrating the phenomenon of aggregation-induced emission (AIE). Its emission can be reversibly switched between blue and dark states by repeated protonation and deprotonation. Such behaviour enables it to work as a fluorescent pH sensor in both solution and the solid state and as a chemosensor for detecting acidic and basic organic vapors. Analyses by NMR spectroscopy, single-crystal X-ray diffraction and computational calculations suggest that the change in electron affinity of the pyridinyl unit and molecular conformation of CP_3E upon protonation and deprotonation is responsible for such sensing processes.

Introduction

pH is critical to all life forms. Only a small change in environmental pH can devastate a number of plant and animal lives. Acidification of soils, streams, lakes and seawater caused by acid rain and excessive human activities and untreated sewage can lead to ecological disaster. The catastrophic consequences of such pollution are the depletion of individual species, reduction in biodiversity, the elimination of specific strains, *etc.* Monitoring the pH level is thus crucial to the preservation of our living environment. Among various analytical techniques, fluorescence (FL)-based methods have attracted special interest because they enjoy superb sensitivity, selectivity, rapidity, portability, *etc.*[1] The main chemical analytes contributing to pH are ionic species existing or functioning in aqueous media. Incongruously, however, most luminescent materials are hydrophobic aromatics that are barely soluble in water. Although their water solubility can be improved by the incorporation of hydrophilic groups, the resulting amphiphilic molecules tend to aggregate when dissolved in water. Aggregation can partially or even completely quench light emission and this aggregation-caused quenching (ACQ) effect has limited the real world applications of many lead luminophores identified by the laboratory solution-screening process in an engineering robust form.[2]

We observed a phenomenon of aggregation-induced emission (AIE) in some propeller-like molecules such as siloles and tetraphenylethenes.[3] Instead of quenching, aggregate formation enhances their light emission, turning them from weak luminophores in solution to strong emitters in the aggregated state. The restriction of intramolecular rotation (IMR) has been found to be the main cause for the AIE effect. Since then, many scientists around the world have worked on the design of new AIE luminogens and explored their practical applications in optoelectronics and sensory systems.[3b,3c,4,5]

Our research team has utilized AIE fluorogens to develop fluorescent pH sensors that sensitively respond to subtle pH changes. For example, a hexaphenylsilole derivative 1,1-bis-[4-(diethylaminomethyl)phenyl]-2,3,4,5-tetraphenylsilole can dissolve readily in acidic aqueous media due to the transformation of its amino groups to ammonium salts.[6] The resulting non-emissive aqueous solution is turned on by increasing the pH value. The working principle involved in the pH sensing process is the dissolution (deaggregation) and aggregation of the AIE luminogen at the appropriate pH value. Following this mechanism, a fluorescent pH sensor with the

[a]*HKUST Shenzhen Research Institute, No. 9 Yuexing 1st RD, South Area, Hi-tech Park, Nanshan, Shenzhen, 518057, China. E-mail: tangbenz@ust.hk*

[b]*Department of Chemistry, Division of Biomedical Engineering, Institute for Advanced Study and Institute of Molecular Functional Materials, The Hong Kong University of Science & Technology, Clear Water Bay, Kowloon, Hong Kong, China*

[c]*Guangdong Innovative Research Team, SCUT-HKUST Joint Research Laboratory, State Key Laboratory of Luminescent Materials and Devices, South China University of Technology, Guangzhou, 510640, China*

† Electronic supplementary information (ESI) available: Experimental procedures, structural characterization data, single crystal data, absorption spectra, molecular orbital amplitude plots, TEM images and particle size analyses. CCDC 928173. For ESI and crystallographic data in CIF or other electronic format see DOI: 10.1039/c3sc50648g

opposite response can be readily designed. Thus, the emission of 1-[2-(4-hydroxyphenyl)ethynyl]pentaphenylsilole, a hydroxylated silole, is switched on and off in the low and high pH regions, as the luminogenic molecules are aggregated and deaggregated (or dissolved) in the acidic and basic aqueous media, respectively.[7] By taking advantage of the AIE effect and chemical reactivity towards OH^- and H^+ ions, a red emissive zwitterionic hemicyanine dye constructed from tetraphenylethene and *N*-alkylated indolium shows different emission colors and intensities at various pH values, and thus works as a fluorescent sensor to follow pH changes in a wide range.[8]

Protonation of some heteroatom-containing groups such as pyridinyl, amino and phenol will significantly change their electron-withdrawing properties. This will have an obvious effect on the emission color or intensity of fluorophores with these pH-sensitive groups. Some fluorescent pH sensors based on the above process have been designed and synthesized but the detection is normally carried out in the solution state due to the ACQ effect.[9] In the pursuit of new AIE materials for application as fluorescent pH sensors, in this edge article, we designed and constructed a heteroatom-containing luminogen (CP_3E, Scheme 1) from diphenylethene, carbazole and pyridine building blocks. CP_3E is AIE-active and displays the feature of intramolecular charge transfer (ICT)[10,11] due to the donor (D)–acceptor (A) interaction between its carbazolyl and pyridinyl units. Its emission can be reversibly switched between blue and dark state by repeated protonation and deprotonation, thus enabling it to work as a fluorescent pH sensor in both the solution and solid states as well as a probe for acidic and basic organic vapors.

Results and discussion

Synthesis

CP_3E was synthesized in a moderate yield according to the synthetic procedures shown in Scheme 1. Briefly, addition of 4-cyanopyridine (**1**) into a lithiated THF solution of bromobenzene followed by hydrolysis in water formed 4-pyridophenone (**2**). Wittig–Horner reaction of **2** with diethyl 4-iodobenzylphosphonate (**3**)[12] in the presence of potassium *tert*-butoxide generated 1-(4-pyridinyl)-1-phenyl-2-(4-iodophenyl)ethene (**4**), which reacted with carbazole to give the designed product as a white powder. CP_3E was characterized by NMR and mass spectroscopies and elemental analysis, which gave satisfactory data corresponding to its molecular structure (see ESI† for details). Single crystals of CP_3E were grown from its hexane–ethyl acetate mixture (3 : 1, v/v) and analyzed crystallographically. The data are provided in Table S1 and S2.†

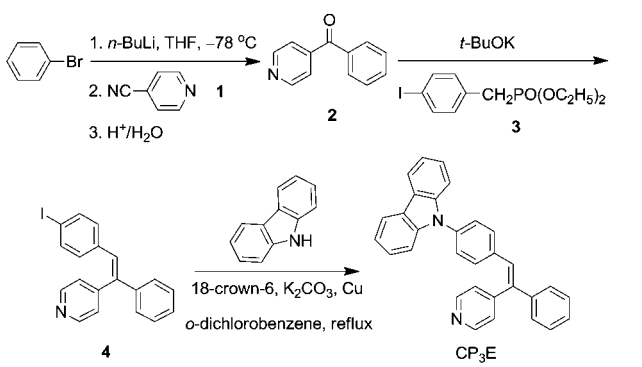

Scheme 1 Synthetic route to CP_3E.

Tunable optical properties

Albeit weak, CP_3E exhibits the ICT phenomenon owing to the presence of electron-donating and accepting units in the molecular structure. As shown in Fig. 1A, the UV spectrum has a peak at 340 nm in hexane, which changes little when the measurement is performed in other solvents with increasing polarity. The solvent polarity also does not exert much influence on its photoluminescence (PL) properties, with the emission maximum and intensity in hexane being 13 nm blue-shifted and half, respectively, from those in acetonitrile, the most polar solvent used for the measurement (Fig. 1B). A Lippert–Mataga plot of Stokes shift against the orientation polarizability of the solvent gives an upward straight line with a small slope, indicative of a weak ICT feature.

Addition of a drop of trifluoroacetic acid (TFA) into a chloroform solution of CP_3E protonates its pyridine unit and generates CP_3EH^+ (Scheme 2). This is proved by the ^1H NMR spectra shown in Fig. 2. The pyridinyl protons (a and b) shift downfield after protonation because of the transformation of the pyridine ring in CP_3E to an electron-deficient pyridinium unit in CP_3EH^+. The resonances of phenyl A and olefin (labeled with "c") protons also move to lower fields for the same reason. The ^1H NMR spectrum is fully restored when an excess of triethylamine (TEA) is injected into the solution, suggesting that the transformation between CP_3E and CP_3EH^+ is completely reversible and non-destructive in nature. Since the ^1H NMR analysis suggests that the pyridinium unit in CP_3EH^+ is a strong electron-accepting group, it is thus anticipated that CP_3EH^+ exhibits a stronger ICT effect but weaker PL than CP_3E in the same solvent. This is indeed the case. As depicted in Fig. S1,† the optical properties of CP_3EH^+, particularly the PL process, are

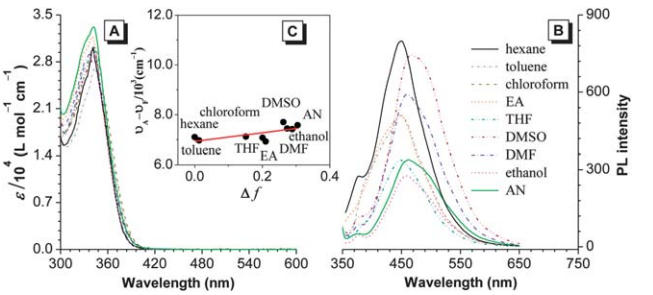

Fig. 1 (A) UV and (B) PL spectra and (C) Lippert–Mataga plot of CP_3E in solvents with different polarities. Concentration: 10 μM; excitation wavelength: 340 nm. Abbreviations: EA = ethyl acetate, THF = tetrahydrofuran, DMSO = dimethyl sulfoxide, DMF = dimethylformamide, AN = acetonitrile. υ_A = absorption wavenumber, υ_F = emission wavenumber and Δf = orientation polarizability = $(\varepsilon - 1)/(2\varepsilon + 1) - (n^2 - 1)/(2n^2 + 1)$, where ε = dielectric constant and n = refractive index.

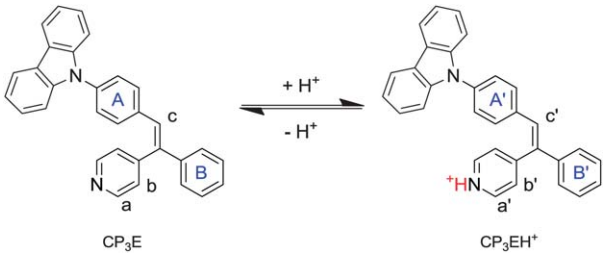

Scheme 2 Reversible transformation between CP_3E and CP_3EH^+ by repeated protonation and deprotonation.

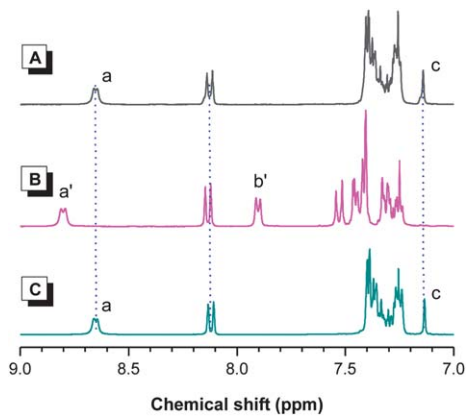

Fig. 2 ^1H NMR spectra of CP_3E in $CDCl_3$ containing (A) 0 and (B) 0.01 mL of trifluoroacetic acid (TFA). The spectrum in (C) was obtained by adding 0.05 mL of triethylamine into (B).

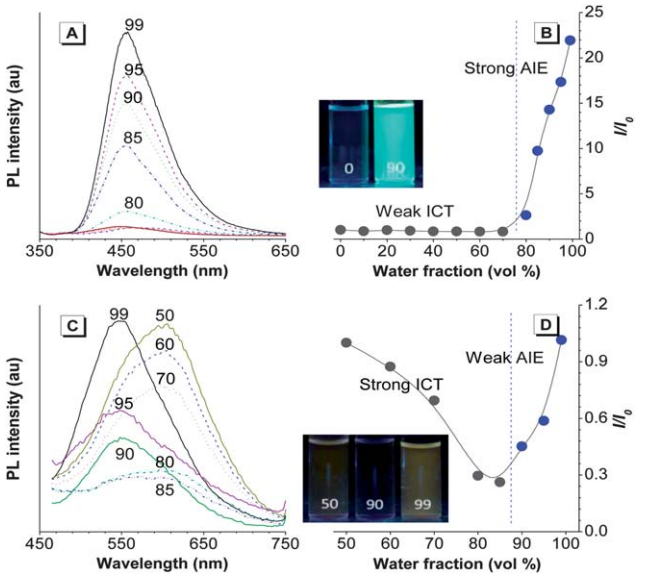

Fig. 3 (A and C) PL spectra of (A) CP_3E in THF–water mixtures and (C) CP_3EH^+ in acidified THF–water mixtures with different water fractions (f_w). (B and D) Change in the relative PL intensity (I/I_0) with the composition of the aqueous mixtures of (B) CP_3E and (D) CP_3EH^+. Insets: fluorescent photos of the aqueous mixtures taken under a 365 nm UV lamp with different f_w values.

more susceptible to the change in solvent polarity. For example, the UV spectrum has a peak at 380 nm in chloroform, which moves to 391 nm when the measurement is carried out in acetonitrile. While CP_3EH^+ emits a yellow PL at 558 nm in chloroform, it becomes a red fluorophore and luminescences weakly at ~640 nm in acetonitrile. Its Stokes shift increases more rapidly on increasing the solvent polarity, further substantiating the discussion above. It is noteworthy that in the same solvent, CP_3E shows redder absorption, which is indicative of its higher conjugation.

Aggregation-induced emission

We then investigated the photophysical properties of both dyes in the aggregated state. The diluted THF solution (10 μM) of CP_3E emits a blue PL at ~455 nm (Fig. 3A). Gradual addition of water into the THF solution slightly red-shifts the PL spectrum as the ICT effect becomes stronger in solvent mixtures with higher polarity. The emission intensity, on the other hand, remains low even when up to 70% of water is added to the THF solution. Afterwards, it rises swiftly. The higher the water fraction (f_w), the stronger is the light emission. From the dilute THF solution to 99% aqueous mixture, the PL intensity increases by ~22-fold. Since CP_3E is insoluble in water, its molecules must have been aggregated in the presence of a large amount of water. However, all the aqueous mixtures are homogenous without precipitates, suggesting that the aggregates are of nano-dimensions. This is proved by the level-off tail observed in the UV spectrum in the longer wavelength region in aqueous mixtures with high f_w values (Fig. S2A†). Analyses by particle size analyzer and transmission electronic microscopy also reveal the formation of nanoaggregates with diameters in the range of 100–200 nm (Fig. S2B†). Clearly, aggregate formation has enhanced the PL of CP_3E or, in other words, it is AIE-active. As discussed before, CP_3E is a weak ICT dye. Thus, even as the polarity of the solvent mixture becomes higher with gradual addition of water into the THF solution, its photophysical properties are little affected. On the other hand, the active rotation of the periphery aryl rings has consumed the energy of the excitons. Thus, although CP_3E is emissive in THF and THF–water mixtures with low water fractions, the intensity is relatively weak. At f_w > 70%, aggregates form, which restricts the IMR process and blocks the nonradiative relaxation channels[13] due to the stabilization of the molecular conformation by multiple C–H···π hydrogen bonds (Fig. S3†). Meanwhile, the twisted conformation of the dye molecule has effectively hampered the formation of detrimental species such as excimers by strong intermolecular interaction.[14] All these collectively make CP_3E a strong emitter in the aggregated state.

CP_3EH^+, on the other hand, displays distinctly different emission behaviour. From the disappearance of the absorption peak at ~350 nm, complete protonation of CP_3E to CP_3EH^+ was achieved only in acidified THF–water mixtures with 50% or higher water content (Fig. S4A†). Thus, we investigated the PL of CP_3EH^+ in aqueous mixtures with f_w values larger than 50%. As the polarity of the aqueous mixture and hence the ICT effect become higher and stronger with progressive addition of water

into the 50% aqueous mixture, the PL of CP_3EH^+ is weakened gradually (Fig. 3C). At f_w > 85%, aggregates form, which activates the AIE process and hence makes the solvent mixture emissive again. The magnitude of emission induction is, however, limited as the PL intensity in 99% aqueous mixture is basically the same as that at 50% water content (Fig. 3D). The PL maximum is located at shorter wavelength, presumably due to the decrease in the solvent effect on the photophysical properties of the aggregates. The size of the nanoaggregates determined by zeta potential analyzer is 30–50 nm (Fig. S4B†), which is much smaller than that of CP_3E as CP_3EH^+ is less hydrophobic and thus can still dissolve in aqueous mixtures with high water contents.

pH sensing

The AIE effect of CP_3E and its reversible transformation between the bright neutral state and dim cationic form by repeated protonation and deprotonation encouraged us to explore its application as a fluorescent pH sensor. As shown in Fig. 4A, the PL spectrum of CP_3E in THF–buffer mixture (3 : 7, v/v) at pH 1 is almost a flat line parallel to the abscissa because of its transformation to the weakly emissive CP_3EH^+ under such acidic conditions. The spectrum was intensified when the pH was increased from 1 to 4 because of the progressive decrease in the population of CP_3EH^+ in solution (Fig. 4B). At pH > 4, the CP_3E molecules are less likely to undergo protonation and its emission thus remains unaltered. The fluorescent photos of the solutions shown in the insets also demonstrate the same phenomenon. The extent of transformation of CP_3E to CP_3EH^+ at different pH values can also be followed by UV analysis (Fig. S5A†). At pH 1–2, CP_3EH^+ is predominant in solution and absorbs at ~400 nm. The absorption is weakened progressively with increasing pH. Meanwhile, a new peak owing to the absorption of CP_3E appears at ~350 nm. At pH 4, a weak absorption tail is still observed at the longer wavelength region but disappears completely at pH 5, suggesting that no protonation occurs at such a pH value. The spectra measured at higher pH are basically the same as that at pH 5.

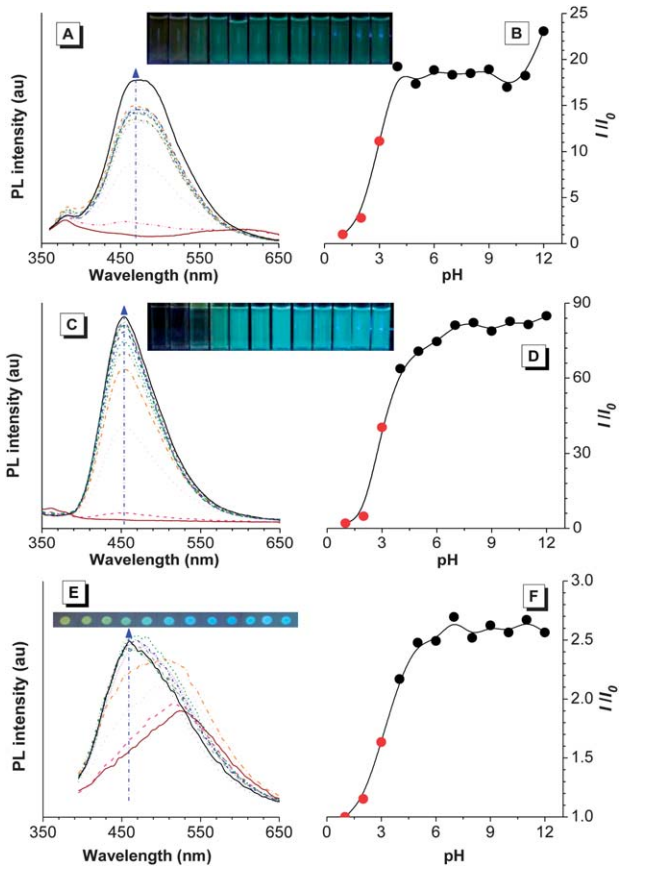

Fig. 4 Effect of pH on the (A, C and E) PL spectra and (B, D and F) relative PL intensity (I/I_0) of CP_3E in (A and C) THF–buffer mixtures with volume ratios of (A) 3 : 7 and (C) 1 : 9 and (E) deposited on filter paper. Insets in (A, C and E): fluorescent photos at pH 1 (left) to 12 (right) taken under 365 nm UV irradiation.

The detection can also be performed in the aggregated state. Since CP_3E is hydrophobic in nature, it will form aggregates in a THF–buffer mixture with 90% water content. At pH 1–2, it will protonate to form CP_3EH^+ that possesses lower hydrophobicity but a stronger ICT effect, thus rendering the solution almost non-emissive (Fig. 4C). The emission was turned on again with increasing magnitude when the pH was increased progressively from 2 to 7 because most of the CP_3E molecules are not protonated, as demonstrated by the appearance of a strong absorption peak at ~350 nm in the UV spectrum (Fig. S5B†). Afterwards, the PL intensity remains almost constant. From pH 1 to 12, the emission is enhanced by more than 80-fold, which is much higher than that in the solution state (Fig. 4D). Evidently, the nanoaggregates work as a more sensitive pH sensor than their isolated species in solution, thanks to their AIE feature.

For real-world applications, it is preferable to perform the detection on solid supports because this requires no complex and expensive equipment and is thus simple, quick and convenient.[15] In such regard, we deposited CP_3E on filter paper and checked its PL after addition of several drops of buffer solutions of different pH. The untreated strip emits bright blue PL upon photoexcitation (inset in Fig. 4E). Addition of acidic buffer solutions (pH 1 or 2) weakens the PL and changes the emission color to yellow. In contrast, the paper strips give blue light at pH 3 and 4 but the intensity is not as strong as that of the untreated one. At pH > 4, no difference in the emission intensity was basically observed between the CP_3E-loaded strips as the dye exists predominantly in its neutral form. Instead of visual observation, we also measured their PL using a spectrophotometer and obtained results similar to those obtained in the solution and aggregated states (Fig. 4E and F).

Since the PL of CP_3E is pH-sensitive, we can make use of such a property to utilize it as a fluorescent sensor for the detection of volatile organic compounds with high acidity and basicity.[16] Due to its strong mechanical strength, we utilized a thin-layer chromatography (TLC) plate as a solid support. The dye-loaded plate emits a greenish-yellow light due to the partial transformation of CP_3E to CP_3EH^+ by the weak acidity of the silica gel (Fig. 5A). After fuming with TFA vapour, the dye spot turns red and emits weakly. It, however, converts back to its blue emissive neutral form when treated with TEA vapour. The switch between the weakly emissive and bright blue states can be repeated

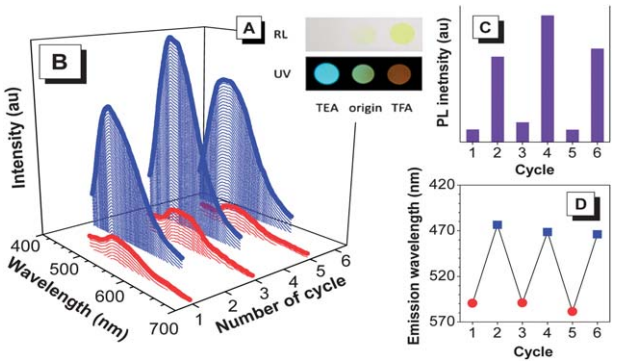

Fig. 5 (A) Photos of CP_3E spots on a TLC plate before (central) and after fuming with (left) TEA and (right) TFA vapors. The photos were taken under normal room lighting (RL) and UV illumination (365 nm). Change in the PL (B) spectrum, (C) intensity and (D) wavelength of a CP_3E spot deposited on a TLC plate by repeated fuming with TFA and TEA vapors.

many times without fatigue by alternately fuming with TEA and TFA vapors as the process is non-destructive in nature (Fig. 5B–D).

Miscellaneous applications

Instead of a fluorescent pH sensor, we also explored the high-tech applications of CP_3E in other fields. We found that CP_3E can work as a fluorescent visualizer for intracellular imaging. As depicted in Fig. 6, the AIE-active CP_3E selectively stains the cytoplasmic regions of living HeLa cells. Bright blue light was observed from the lipid droplets, presumably due to the hydrophobic nature of the CP_3E molecules, which favors their accumulation on these biomacromolecules. We are currently utilizing CP_3E to sense pH inside the living cells and the details will be presented in the future.

Mechanism

The above discussion states that CP_3E and CP_3EH^+ possess distinctly different photophysical properties. While it is proven that the different electron-accepting abilities of the pyridine and pyridinium units contribute to different ICT effects in CP_3E and CP_3EH^+, what causes the change in the AIE feature? We believe the molecular conformation plays a crucial role. The single-crystal structure of CP_3E provided in Fig. 7 shows that the molecule adopts a twisted conformation due to the steric effect between the aryl rings. After protonation, its conformation

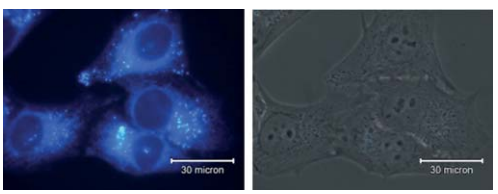

Fig. 6 (Left) Fluorescent and (right) bright-field images of HeLa cells stained with CP_3E for 2 h.

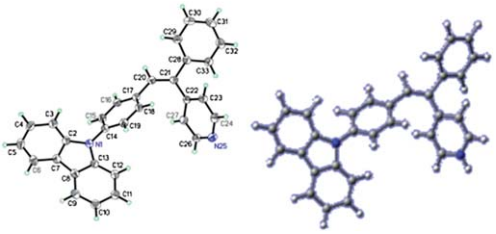

Fig. 7 (Left) Single-crystal structure of CP_3E and (right) optimized structure of CP_3EH^+ obtained by Gaussian 03, B3LYP/6-31+G** basis set.

becomes more planar, as revealed by the optimized structure of CP_3EH^+ obtained by theoretical calculations. The selected bond lengths and dihedral angles summarized in Table S3† also support this speculation. Whereas the pyridine and phenyl A rings twist from the vinyl core by 51.7° and 40.8°, respectively, the amplitude becomes smaller in CP_3EH^+ (34.2° and 26.6°). This implies better electronic communication in CP_3EH^+, thus shortening the single bonds connecting the components and imparting CP_3EH^+ with a high conjugation and hence a smaller energy band gap (Fig. S6†). Previous studies have shown that molecules with a more flat conformation enjoy higher electronic conjugation and lower potential energy.[3e] Thus, they are less likely to undergo intramolecular rotation even when they contain rotatable aromatic rings. As the restriction of the IMR process is mainly responsible for the AIE phenomenon, the relatively low tendency of intramolecular rotation in CP_3EH^+ due to its more planar conformation should, in most cases, lead to a weaker AIE effect.

Conclusions

In this work, a heteroatom-containing organic fluorophore (CP_3E) was designed and synthesized from carbazole, pyridine and diphenylethene building blocks. CP_3E exhibits an ICT effect caused by the D–A interaction between its carbazole and pyridine units. Whereas it emits faintly in solution, it becomes highly emissive in the aggregated state, demonstrating the AIE phenomenon. Its emission can be reversibly switched between blue and dark states by repeated protonation and deprotonation. Such behaviour enables it to work as a fluorescent pH sensor in both the solution and solid states and a chemosensor for detecting volatile organic compounds with high acidity and basicity. CP_3E can selectively stain the cytoplasmic regions of living cells. Analyses by NMR spectroscopy, single-crystal X-ray diffraction and theoretical calculations suggest that the change in electron affinity of the pyridinyl moiety and molecular conformation upon protonation/deprotonation is responsible for the sensing process. Thus, introduction of an AIE unit to the traditional pH sensitive fluorophores is an efficient route to expand their practical useful application from solely solution to both solution and solid states. Such results also provide valuable information on the future design of new fluorescent probes, whose light-emitting behaviours can be readily tuned by simply varying the environmental conditions.

Acknowledgements

The work reported in this edge article was partially supported by the National Basic Research Program of China (973 Program; 2013CB834701), the Research Grants Council of Hong Kong (HKUST2/CRF/10 and N_HKUST620/11), and the University Grants Committee of Hong Kong (AoE/P-03/08). B. Z. Tang thanks the Guangdong Innovative Research Team Program (201101C0105067115) for support.

Notes and references

1 (*a*) A. P. Desilva, H. Q. N. Gunaratne, T. Gunnlangsson, A. J. M. Huxley, C. P. Mccoy, J. T. Rademacher and T. E. Rice, *Chem. Rev.*, 1997, **97**, 1515; (*b*) W. P. Ambrose, P. M. Goodwin, J. H. Jett, A. Van Orden, J. H. Werner and R. A. Keller, *Chem. Rev.*, 1999, **99**, 2929; (*c*) W. F. Patton, *BioTechniques*, 2000, **28**, 944.

2 (*a*) S. W. Thomas III, G. D. Joly and T. M. Swager, *Chem. Rev.*, 2007, **107**, 1339; (*b*) C. T. Chen, *Chem. Mater.*, 2004, **16**, 4389; (*c*) M. Grell, D. D. C. Bradley, G. Ungar, J. Hill and K. S. Whitehead, *Macromolecules*, 1999, **32**, 5810; (*d*) R. Jakubiak, C. J. Collison, W. C. Wan and L. Rothberg, *J. Phys. Chem. A*, 1999, **103**, 2394; (*e*) M. Grell, D. D. C. Bradley, X. Long, T. Chamberlain, M. Inbasekaran, E. P. Woo and M. Soliman, *Acta Polym.*, 1998, **49**, 439; (*f*) U. Lemmer, S. Heun, R. F. Mahrt, U. Scherf, M. Hopmeier, U. Siegner, E. O. Gobel, K. Müllen and H. Bassler, *Chem. Phys. Lett.*, 1995, **240**, 373.

3 (*a*) J. D. Luo, Z. L. Xie, J. W. Y. Lam, L. Cheng, H. Y. Chen, C. F. Qiu, H. S. Kwok, X. W. Zhan, Y. Q. Liu, D. B. Zhu and B. Z. Tang, *Chem. Commun.*, 2001, 1740; (*b*) Y. N. Hong, J. W. Y. Lam and B. Z. Tang, *Chem. Commun.*, 2009, 4332; (*c*) Y. N. Hong, J. W. Y. Lam and B. Z. Tang, *Chem. Soc. Rev.*, 2011, **40**, 5361.

4 (*a*) Z. J. Zhao, P. Lu, J. W. Y. Lam, Z. M. Wang, C. Y. K. Chan, H. H. Y. Sung, I. D. Williams, Y. G. Ma and B. Z. Tang, *Chem. Sci.*, 2011, **2**, 672; (*b*) Z. Y. Yang, Z. G. Chi, T. Yu, X. Q. Zhang, M. N. Chen, B. J. Xu, S. W. Liu, Y. Zhang and J. R. Xu, *J. Mater. Chem.*, 2009, **19**, 5541; (*c*) C. Y. K. Chan, Z. J. Zhao, J. W. Y. Lam, J. Z. Liu, S. M. Chen, P. Lu, F. Mahtab, X. J. Chen, H. H. Y. Sung, H. S. Kwok, Y. G. Ma, I. D. Williams, K. S. Wong and B. Z. Tang, *Adv. Funct. Mater.*, 2012, **22**, 378; (*d*) Z. J. Zhao, J. W. Y. Lam, C. Y. K. Chan, S. M. Chen, J. Z. Liu, P. Lu, M. Rodriguez, J. L. Maldonado, G. Ramos-Ortiz, H. H. Y. Sung, I. D. Williams, H. M. Su, K. S. Wong, Y. G. Ma, H. S. Kwok, H. Y. Qiu and B. Z. Tang, *Adv. Mater.*, 2011, **23**, 5430; (*e*) Z. J. Zhao, Z. M. Wang, P. Lu, C. Y. K. Chan, D. D. Liu, J. W. Y. Lam, H. H. Y. Sung, I. D. Williams, Y. G. Ma and B. Z. Tang, *Angew. Chem., Int. Ed.*, 2009, **48**, 7608.

5 (*a*) S. J. Chen, J. Z. Liu, Y. Liu, H. M. Su, Y. N. Hong, C. K. W. Jim, R. T. K. Kwok, N. Zhao, W. Qin, J. W. Y. Lam, K. S. Wong and B. Z. Tang, *Chem. Sci.*, 2012, **3**, 1804; (*b*) Z. G. Chi, X. Q. Zhang, B. J. Xu, X. Zhou, C. P. Ma, Y. Zhang, S. W. Liu and J. R. Xu, *Chem. Soc. Rev.*, 2012, **41**, 3878; (*c*) Y. N. Hong, L. M. Meng, S. J. Chen, C. W. T. Leung, L. T. Da, M. Faisal, D. A. Silva, J. Z. Liu, J. W. Y. Lam, X. H. Huang and B. Z. Tang, *J. Am. Chem. Soc.*, 2012, **134**, 1680; (*d*) Y. N. Hong, H. Xiong, J. W. Y. Lam, M. Haussler, J. Z. Liu, Y. Yu, Y. C. Zhong, H. H. Y. Sung, I. D. Williams, K. S. Wong and B. Z. Tang, *Chem.–Eur. J.*, 2010, **16**, 1232.

6 Y. Q. Dong, J. W. Y. Lam, A. Qin, Z. Li, J. Liu, J. Sun, Y. P. Dong and B. Z. Tang, *Chem. Phys. Lett.*, 2007, **446**, 124.

7 Z. Li, Y. Q. Dong, J. W. Y. Lam, J. Sun, A. Qin, M. Häußler, Y. P. Dong, H. H. Y. Sung, I. D. Williams, H. S. Kwok and B. Z. Tang, *Adv. Funct. Mater.*, 2009, **19**, 905.

8 S. Chen, J. Liu, Y. Liu, H. Su, Y. Hong, C. K. W. Jim, R. T. K. Kwok, N. Zhao, W. Qin, J. W. Y. Lam, K. S. Wong and B. Z. Tang, *Chem. Sci.*, 2012, **3**, 1804.

9 (*a*) J. Han and K. Burgess, *Chem. Rev.*, 2010, **110**, 2709; (*b*) T. Jokic, S. M. Borisov, R. Saf, D. A. Nielsen, M. Kühl and I. Klimant, *Anal. Chem.*, 2012, **84**, 6723; (*c*) B. Tang, F. Yu, P. Li, L. Tong, X. Duan, T. Xie and X. Wang, *J. Am. Chem. Soc.*, 2009, **131**, 3016; (*d*) T. Myochin, K. Kiyose, K. Hanaoka, H. Kojima, T. Terai and T. Nagano, *J. Am. Chem. Soc.*, 2011, **133**, 3401.

10 (*a*) B. Valeur, *Molecular Fluorescence: Principles and Applications*, Wiley-VCH, Weinheim, Germany, 2002, ch. 3; (*b*) E. Lippert, W. Rettig, V. Bonacic-Koutecky, F. Heisel and J. A. Miehe, *Adv. Chem. Phys.*, 1987, **68**, 1; (*c*) Z. R. Grabowski and K. Rotkiewicz, *Chem. Rev.*, 2003, **103**, 3899.

11 (*a*) J. S. Yang, K. L. Liau, C. Y. Li and M. Y. Chen, *J. Am. Chem. Soc.*, 2007, **129**, 13183; (*b*) S. S. Palayangoda, X. C. Cai, R. M. Adhikari and D. C. Neckers, *Org. Lett.*, 2008, **10**, 281; (*c*) M. S. Yuan, Z. Q. Liu and Q. Fang, *J. Org. Chem.*, 2007, **72**, 7915; (*d*) S. Cogan, S. Zilberg and Y. Haas, *J. Am. Chem. Soc.*, 2006, **128**, 3335; (*e*) E. Lippert, W. Luder, F. Moll, W. Magele, H. Boos, H. Prigge and I. Seibold-Blankenstein, *Angew. Chem.*, 1961, **73**, 695; (*f*) S. Luis, M. Manuela, O. R. Bjorn and L. Roland, *J. Am. Chem. Soc.*, 1995, **117**, 3189.

12 N. Mizoshita, Y. Goto, T. Tani and S. Inagaki, *Adv. Funct. Mater.*, 2008, **18**, 3699.

13 Q. Peng, Y. Yi, Z. Shuai and J. Shao, *J. Am. Chem. Soc.*, 2007, **129**, 9333.

14 (*a*) C. J. Bhongale and C. S. Hsu, *Angew. Chem., Int. Ed.*, 2006, **45**, 1404; (*b*) M. R. Han and M. Hara, *New J. Chem.*, 2006, **30**, 223; (*c*) C. Yuan, X. Tao, Y. Ren, Y. Li, J. Yang, W. Yu, L. Wang and M. Jiang, *J. Phys. Chem. C*, 2007, **111**, 12811; (*d*) J. Chen and Y. Cao, *Macromol. Rapid Commun.*, 2007, **28**, 1714; (*e*) Y. T. Lee, C. L. Chiang and C. T. Chen, *Chem. Commun.*, 2008, 217.

15 (*a*) A. Leino and B. M. Loo, *Ann. Clin. Biochem.*, 2007, **44**, 563; (*b*) W. Putalun, H. Tanaka and Y. Shoyama, *Phytochem. Anal.*, 2005, **16**, 370.

16 (*a*) E. S. Snow, F. K. Perkins, E. J. Houser, S. C. Badescu and T. L. Reinecke, *Science*, 2005, **307**, 1942; (*b*) J. Janata and M. Josowicz, *Nat. Mater.*, 2003, **2**, 19.

